FOPID Based LFC in a Smart Interconnected Power System Including Wind Turbine and Electric Vehicles

H. Shayeghi, M. Mohammadzadeh, S.J. Seyed-Shenava and R. Dadkhah Doltabad

***Abstract*— This paper presents a Fractional Order PID (FOPID) controller optimized using Ant Lion Optimizer (ALO) algorithm to Load Frequency Control (LFC) and optimal control State-of-Charge (SOC) of a smart interconnected power system in the presence of wind turbine and Plug-in Hybrid Electric Vehicles (PHEVS). In this regard, PHEVS with the capability of connecting to grid (V2G) in addition to reduce dependence of power system to thermal units, can perform a vital role in reducing the frequency fluctuation caused by intermittent power generation by wind turbine. On the other hand, by increasing connection of V2G, the need to investigate the balance of LFC is felt more than ever. The battery state-of-charge (SOC) is controlled by the optimized SOC deviation control. Main control parameters of the FOPID controller are control gains, fractional orders of integrator and derivative which improve its performance comparison to Proportional-Integral (PI) controller. In addition, to achieve the best performance in the smart interconnected power system, tuning of these parameters is essential. So, we have used ALO algorithm in order to optimal tuning of the FOPID based LFC controller. The ALO mimics the hunting mechanism of ant lions in nature. The simulation results show that the proposed controller has good performance from the perspective of overshoot/ undershoot and settling time in comparison with PI controller in order to significantly reduce the frequency fluctuations in the presence of V2G.**

***Keywords*— Load frequency control, FOPID, State-of-charge, V2G, Ant lion optimizer.**

I. INTRODUCTION

In recent years, by using a wide range of renewable energy sources such as wind turbines, innovative ideas on applying PHEVS and how to use customers of PHEVS has created new developments in the power grid infrastructure. In this regard, renewable energy sources require large scale energy storage for achieving stability of grid frequency [1]. On the other hand, in the future transportation system, the PHEVs are used widely for driving in the customer side because of low-cost charging, reduced petroleum usages and reduced greenhouse emissions [2-3]. However, the wind power is intermittent in nature. This may cause an imbalance of supply and load demand and lead to a severe frequency oscillation problem [4]. Particularly, this problem may occur considerably when the capacity of LFC is insufficient during the night period [5]. For example, according to the energy projects contracts in the United States, approximately 1 million PHEV will be marketed by 2015 and about 425,000 PHEV sold in 2015 [6]. The V2G power control can be applied to compensate for the LFC capacity in the night time [7-8]. Therefore, large scale integration of electric vehicles (EV) and plug-in hybrid vehicles (PHV) for the transportation system brings large capacity of V2G [9]. In [10], the way for tuning the load frequency control signal was presented according to the response speed and the controllable capacity. However, all EVs joining in load frequency control were assumed to have 0.85 SOC, thus performance charging demands of the EV customers was not considered [11].

This paper focuses on load frequency control in the smart interconnected power system. ALO technique is used for optimal tuning of FOPID controller in order to reduce frequency fluctuation in the smart grid system. Also, Battery SOC is managed by using SOC balance control. The simulation results show that the proposed controller has good performance from the perspective of overshoot/undershoot and settling time in comparison with PI controller in order to significantly reduce the frequency fluctuations in the presence of V2G. Also, with the proposed method battery SOC in the V2G will be balance around the 50% in the area 1 and the initial SOC and target SOC in area 2 are faster set at 20% and 90%, respectively than the PI controller. Finally, we have shown the superiority of the control procedure in the scenarios occurs in power system.

II. SYSTEM MODELING

Figure 1 shows a smart interconnected power system including large wind farms, thermal power plant, load, LFC and V2G in the both area.

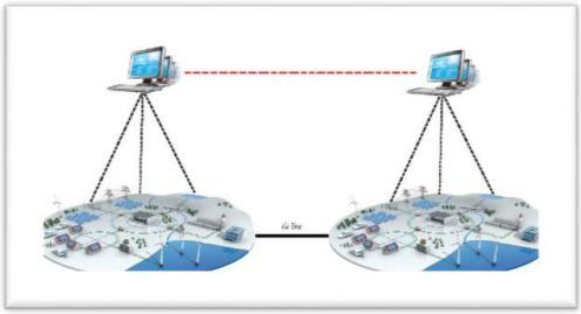

Fig. 1. A smart two area interconnected power system.

Manuscript received May. 18, 2017.

H. Shayeghi, M. Mohammadzadeh and S.J. Seyed-Shenava are with the Electrical Engineering Department, University of Mohaghegh Ardabili, Ardabil, Iran (e-mail: hshayeghi@gmail.com, hashayanfar@gmail.com, masoud.m25869@gmail.com, seyedshenava@uma.ac.ir).

R. Dadkhah Doltabad is with the Electrical Engineering Department, Technical and Vocational University, Technical and Vocational Institute Razi, Ardabil, Iran (e-mail: r.dadkhahdolatabad@gmail.com).

According to sudden power change of intermittent wind power and load fluctuations, thermal generators may be enough power because it does not compensate slow dynamic response [12]. The fast-dynamic response of the vehicle battery based multiple PHEVs is largely expected to compensate LFC task in addition to real-power unbalance in the system when capacity is insufficient. Block diagram of the linearized dynamic model of the smart 2-area interconnected power system is shown in Fig. 2.

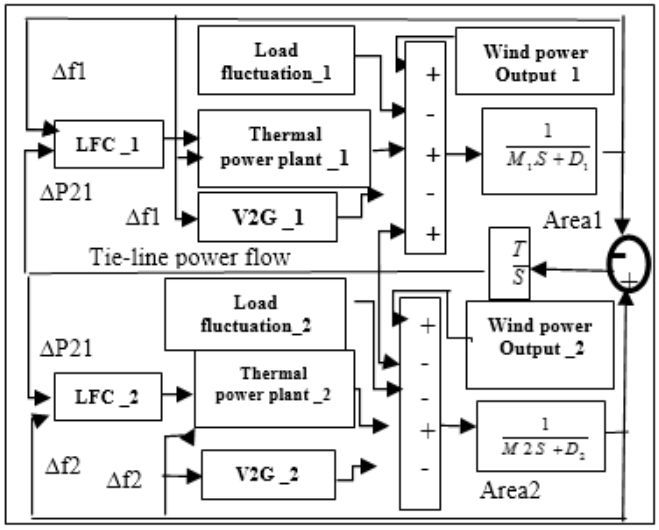

Fig. 2. Linearized model of the smart 2-area interconnected power system.

The models of LFC, thermal power plant, and V2G are shown in Figs. 3, 4, and 5, respectively. In the V2G model, the transfer function for calculation delay is approximately represented by the first-order transfer function with the time delay (T_{PHEV}). The parameters for system, battery model and V2G control are provided in [13].

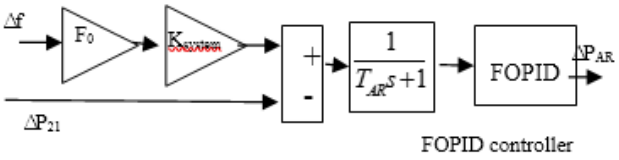

Fig. 3: LFC model.

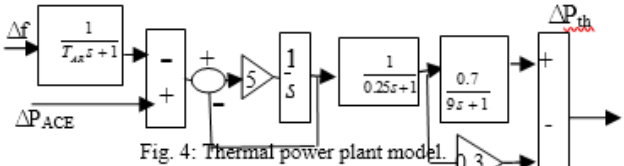

Fig. 4: Thermal power plant model.

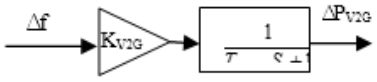

Fig. 5. V2G model

III. V2G POWER CONTROL

Diagram characteristic PHEV power control against frequency deviation is shown in Fig. 6 [13]. The PHEV power output is controlled as the droop characteristics against the frequency deviation. The active V2G power (PV2G) injected in to the grid is designed according to the self-terminal frequency deviation (Δf) as:

$$P_{V2G} = \begin{cases} K_{V2G}.\Delta f & |K_{V2G}.\Delta f| \le P_{max} \\ P_{max} & K_{V2G}.\Delta f \ge P_{max} \end{cases} \quad (1)$$

Where, K_{V2G} is the V2G gain, Δf is the change of system frequency and P_{MAX} is the maximum V2G power which is limited by the specification of the home outlets. The K_{V2G} can be designed as the function of the maximum PHEV gain (K_{MAX}). In this case, the SOC is balance around the specified level, the K_{V2G} with the SOC balance control proposed in [14] can be defined as:

$$K_{V2G} = K_{max}\left[1-\left(\frac{SoC - SoC_{low(high)}}{SoC_{max(min)} - SoC_{low(high)}}\right)^{n}\right] \quad (2)$$

Where, SOC_{low} and SOC_{high} are the low and high battery SOC, respectively, SOC_{min} and SOC_{max} are the minimum and maximum battery SOC, respectively, and n is the specification of the designed battery SOC. Also, the V1G power is calculated by: Where, K_{max} is the maximum V2G gain.

The V1G is the one-way charging power control from grid to vehicles. The V1G power is calculated by

$$P_{V1G} = \begin{cases} K_{V2G}.\Delta f & 0 < K_{max}\Delta f \le P_{max} \\ P_{max} & P_{max} < K_{max}\Delta f \\ 0 & K_{max}\Delta f \le 0 \end{cases} \quad (3)$$

Where, P_{MAX} is the maximum V2G power which is limited by the specification of the home outlets.

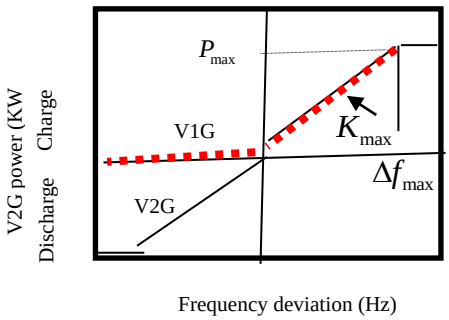

Fig.6. PHEV power control against frequency deviation.

A. SOC deviation control

The SOC can be controlled by the SOC balance control as shown in Fig. 7. Based on (1) and (2), P_{PHEV} can be controlled by tuning the gain K_{V2G} against the frequency deviation. can be adjusted by the SOC deviation control within the specified SOC range.

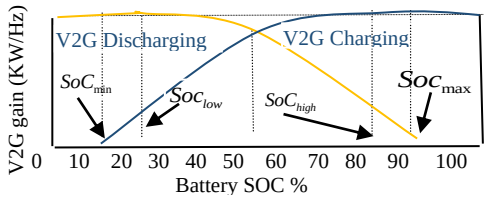

Fig.7. SOC Balance Control.

IV. FOPID CONTROLLER DESIGN FOR LFC PROBLEM

A. Ant lion optimization

Ant lion optimization (ALO) algorithm mainly inspired from the ant lion's larvae natural foraging manner. What happens between ant lions and ants in the trap is simulated via ALO algorithm [15]. Ants move through the search space and at the same time ant lines utilizing traps start to hunting the ants regarding their fitness to trap. In order to model walking method of ants through the search space which is same as searching for food in the nature, the following random method is applied:

$$X(iter) = [0,\ cumsum(2r(1)-1),\ cumsum(2r(2)-)-1,.,cumsum(2r(n)-)-1)] \quad (4)$$

Where, cumsum calculates the cumulative sum, n is the maximum number of iteration, i_{ter} shows the iteration of random walk, and r (t) is a stochastic function defined as follows:

$$r(x) = \begin{cases} 1, & rand \rangle 0.5 \\ 0, & rand \langle 0.5 \end{cases} \quad (5)$$

The position of ants and their related objective functions are saved in the matrices M_{ant} and, MOA respectively. In addition to ants, it is assumed that the ant lions are also hiding somewhere in the search space. In order to save their positions and fitness values, $M_{antlion}$ and MOA matrices are utilized. The pseudo codes the ALO algorithm are defined as follows.

Step 1: Initialize the first population of ants and ant lions randomly. Calculate the fitness of ants and ant lions.

Step 2: Find the best ant lions and assume it as the elite. In this study, the best ant lion obtained so far in each iteration is saved and considered as an elite.

Step 3: For each ant, select an ant lion using Roulette wheel and

a) Create a random walk using Eq. (4)

b) Normalize them in order to keep the random walks inside the search space

$$X_i^t = \frac{(x_i^t - a_i)*(d_i - c_i^t)}{(d_i^t - a_i)} + c_i \quad (6)$$

c) Update the position of ant

$$Ant_i^{iter+1} = \frac{R_A^{iter} + R_E^{iter}}{2} \quad (7)$$

d) Update c and d using the following equations

$$C^{iter+1} = \frac{c^{iter}}{I}, \quad D^{iter+1} = \frac{d^{iter}}{I}, \quad 10^w = \frac{t}{T} \quad (8)$$

Where:

and w is a constant defined based on the current iteration (w = 2 when $i_{ter} > 0.1n$, w = 3 when $i_{ter} > 0.5n$, w = 4 when $i_{ter} > 0.75n$, w = 5 when $i_{ter} > 0.9n$, and w = 6 when $i_{ter} > 0.95n$).

Step 4: Calculate the fitness of all ants.

Step 5: Replace an ant lion with its corresponding ant it if becomes fitter.

Step 6: Update elite if an ant lion becomes fitter than the elite.

Step 7: Repeat from step 3 until stopping criteria is satisfied.

B. FOPID controller

Recently, the FOPID controller has been used in various applications by replacing the fractional order instead of the integer order of derivative and integrator operator, the PI controller has been extended to the $PI^{\alpha}D^{\beta}$ controller that is known as FOPID controller [16]. The following mathematical structure of the FOPID controller is applied:

$$C(S) = K_P + K_I \frac{1}{S^{\alpha}} + K_D S^{\beta} \quad (9)$$

where, the K_P, K_I and K_D are proportional, integral and differential gains and the α and β are fractional order of integrator and derivative, respectively.

C. Objective function

For optimal tuning of the controller parameters choosing the appropriate objective function is necessary to reduce the frequency deviation rapidly. Thus, the proposed approach employs ALO algorithm to solve this optimization problem and search for an optimal or near optimal set of controller parameters. The optimization of the controller parameters is carried out by evaluating the ISTSE objective function as given in Eq. (10). The ISTSE objective function, J for ALO is taken as to minimize the frequency deviations in areas 1 and 2 as:

$$J = \int_0^{t_{sim}} \left(\sum_{i=1}^{n} (\Delta f_i)^2 + \sum t^2 .(\Delta P_{Tie-line})^2 dt\right) \quad (10)$$

The determined controller parameters and ALO algorithm limitation are given in the Table 1. The optimized value of controller parameters is given in the Table 2.

Table I. ALO Parameters values for PI based LFC

Symbol	Quantity	Value
SearchAgents_no	Number of search agents	20
Max_iter	Maximum number of iterations	50
Dim	Number of variables	10
K_p, K_I and K_D	Upper limit	10
K_p, K_I and K_D	Lower limit	0
α and β	Upper limit	2
α and β	Lower limit	0

Table II. Optimal controller gains

Algorithm ALO	K_{P1}	K_{I1}	K_{D1}	K_{P2}	K_{I2}	K_{D2}	α_1	α_2	B_1	B_2
FOPID	1.3378	5.9326	4.3775	8.6195	4.1509	1.2221	0.9055	0.9195	0.5179	0.5084
PI	10	3.053	-	9.9984	3.025	-	-	-	-	-

V. SIMULATION RESULTS

According simulation studies, it is supposed that the studied smart grid is performed under the random load deviation and wind speed. More details of the studies are provided as follows in Figs. 8 and 9, Also, to test the dynamic response of the PHEV and the thermal generator, it is assumed that the only 3000 MW step increase of wind power in area 1 and the only 1500 MW step increase of load in area 2 are subjected to the system model without and with governor and turbine, respectively.

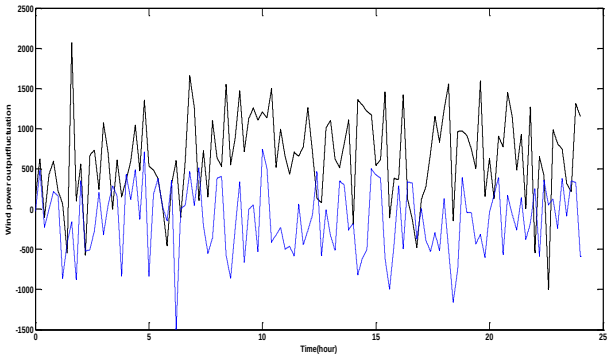

Fig. 8. Wind power output

The frequency deviation under the step increases of wind power and load in the system model without governor and turbine is shown in Figs. 10 and 11, respectively.

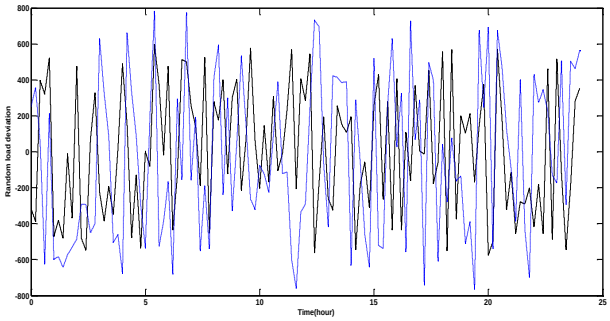

Fig. 9. Random load deviation

As seen in Figs. 10 and 11, the peak values of frequency oscillation in area 1 and area 2 under the V2G control based PHEVs can be highly suppressed in comparison with those of no PHEV. In addition, in the Figs. 10 and 11 both area 1 and 2 show that using the PHEVS reduces the system frequency deviation approximately from 0.07 to 0.05 Hz. Also, the frequency deviation under the step increases of wind power and load in the system model with governor and turbine is illustrated in Figs. 12 and 13, respectively. It can be see that ALO based FOPID controller is compared with the PI controller. These controllers are used to reduce the steady state error based on overshoot/undershoot and settling time.

In order to investigate the control of the V2G based PHEVs and the LFC, applied to compensate the real power unbalance in the studied system. The simulation results is shown in Fig. 15 and 16, 17 respectively. Thus, the frequency deviation between areas with the ALO algorithm based FOPID controller and state of charge V2G is reduced than the ALO algorithm based PI controller.

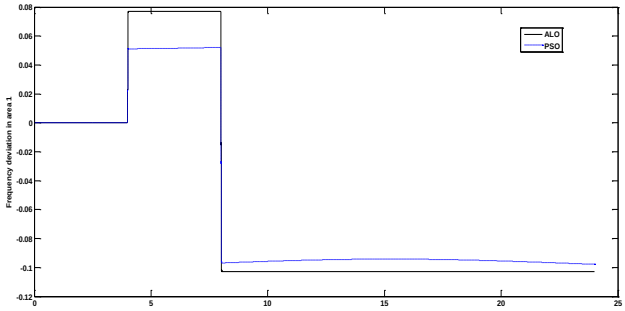

Fig. 10. Frequency deviation in area 1.

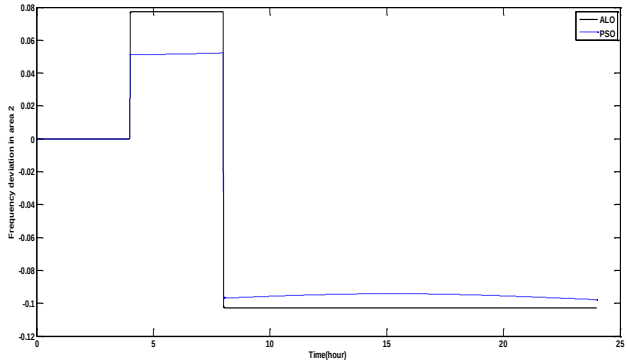

Fig. 11. Frequency deviation in area 2.

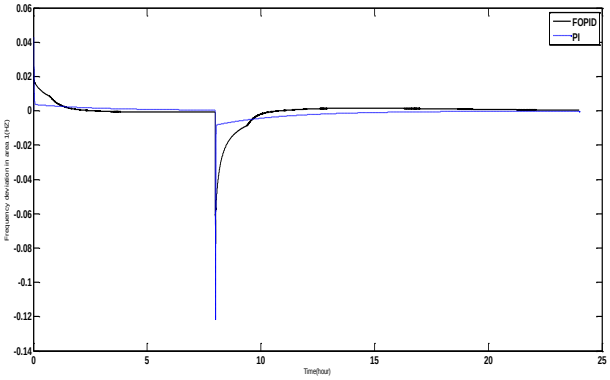

Fig. 12. Frequency deviation in area 1

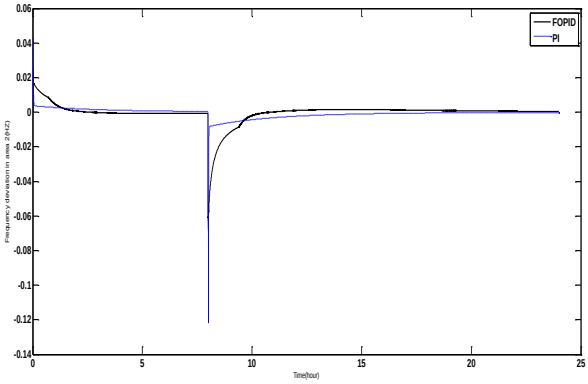

Fig. 13. Frequency deviation in area 2.

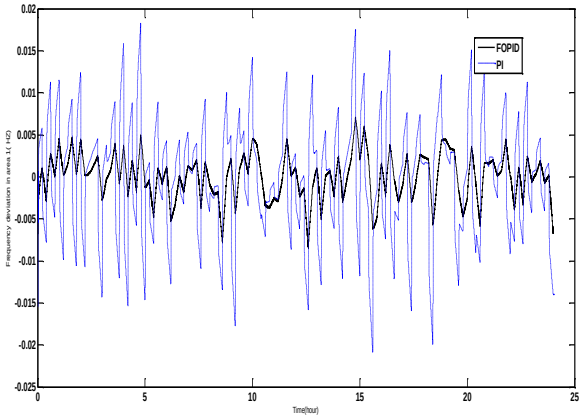

Fig. 15. Frequency deviation in area 1 under the controls of LFC & V2G.

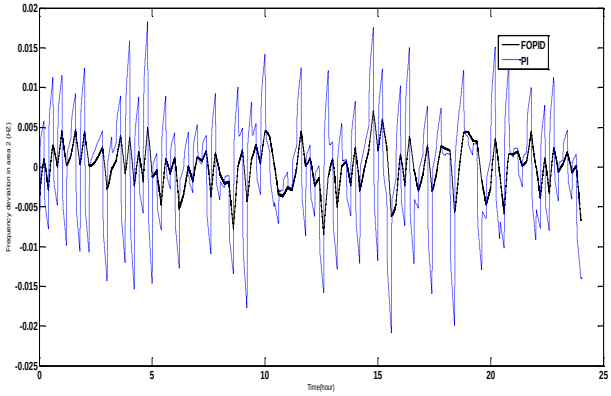

Fig. 16. Frequency deviation in area 2 under the controls of LFC & V2G.

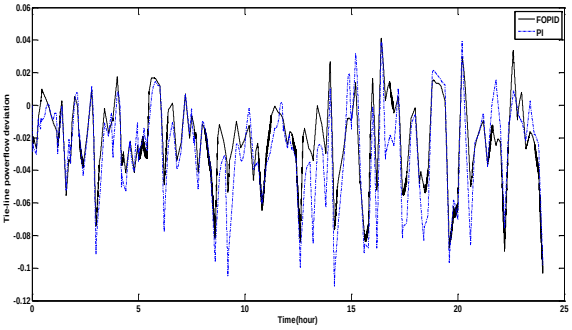

Fig. 17. Tie-line power flow deviation

VI. CONCLUSIONS

Currently, the widespread penetration of large scale wind power has been increasing largely. Accordingly, efforts are made to provide a better control for the smart two-area interconnected power system. We have examined two cases. In case 1, we have investigated the behavior of smart two-area interconnected power system accounting wind power generation and load fluctuation, with and without PHEV. In case 2, the behavior of smart two-area interconnected power system with PHEV including V2G control, random wind power generation, random load and ALO based FOPID controller is analyzed. Simulation results show that V2G control based on PHEV in smart system, reduces the steady-state of frequency to about 40%, comparing to the case which PHEV in not in the grid. Further this work may be extended to multi-area smart power grids with robust control.

APPENDIX

BATTERY MODEL:

The battery SOC is updated as follows:

$$\frac{dsoc}{dt} = \eta I \tag{17}$$

Where η is the efficiency of charge and discharge? Also, the battery CCV (closed circuit voltage) is defined as follows:

$$CCV = V_{nom} + \alpha \frac{RT}{F} \ln\left[\frac{SoC}{C_{nom} - SoC}\right] + R_{\text{int}} I \tag{18}$$

Where R, F, T and R_{int} and are the gas constant, faraday constant, battery temperature and internal resistance, respectively. The system parameters and battery model and V2G control parameters for the system is the following [15].

REFERENCES

[1] Y. Ota, H. Taniguchi, T. Nakajima, K. M. Liyanage, K. Shimizu, T. Masuta, J. Baba, and A. Yokoyama, "Effect of autonomous distributed vehicle-to-grid (V2G) on power system frequency control", Proc. of International Conference on Industrial and Information Systems, pp. 481-485, 2001.

[2] R. Podmore and M. Robinson, "The Role of Simulators for Smart Grid Development", IEEE Transactions on Smart Grid, vol. 1, no. 2, pp. 205-212, 2010.

[3] C. Pang, P. Dutta and M. Kezunovic, "BEVs/PHEVs as Dispersed Energy Storage for V2B Uses in the Smart Grid", IEEE Transactions on Smart Grid, vol. 3, no. 1, pp. 473-482, 2012.

[4] Z. Fan, "A Distributed Demand Response Algorithm and Its Application to PHEV Charging in Smart Grids", IEEE Transactions on Smart Grid, vol. 3, no. 3, pp. 1280-1290, 2012.

[5] E. Sortomme, M. Hindi, S. MacPherson and S. Venkata, "Coordinated Charging of Plug-In Hybrid Electric Vehicles to Minimize Distribution System Losses", IEEE Transactions on Smart Grid, vol. 2, no. 1, pp. 198-205, 2011.

[6] W. Su and M. Chow, "Performance Evaluation of an EDA-Based Large-Scale Plug-In Hybrid Electric Vehicle Charging Algorithm", IEEE Transactions on Smart Grid, vol. 3, no. 1, pp. 308-315, 2012.

[7] Y. Cao, S. Tang, C. Li, P. Zhang, Y. Tan, Z. Zhang and J. Li, "An Optimized EV Charging Model Considering TOU Price and SOC Curve", IEEE Transactions on Smart Grid, vol. 3, no. 1, pp. 388-393, 2012.

[8] A. Yokoyama, "Development of Smarter Grid (I)", The Journal of The Institute of Electrical Engineers of Japan, vol. 130, no. 2, pp. 94-97, 2010.

[9] Sekyung Han, Soohee Han and K. Sezaki, "Development of an Optimal Vehicle-to-Grid Aggregator for Frequency Regulation", IEEE Transactions on Smart Grid, vol. 1, no. 1, pp. 65-72, 2010.

[10] J. A. P. Lopes, F. J. Soares, and P. M. R. Almeida, "Integration of PHEVS in the electric power system", Proc. of IEEE, vol. 99, no. 1, pp. 168–183, 2011.

[11] T. Masuta and A. Yokoyama, "Supplementary Load Frequency Control by Use of a Number of Both Electric Vehicles and Heat Pump Water Heaters", IEEE Transactions on Smart Grid, vol. 3, no. 3, pp. 1253-1262, 2012.

[12] A. Yokoyama, "Development of Smarter Grid (II)", The Journal of The Institute of Electrical Engineers of Japan, vol. 130, no. 3, pp. 163-167, 2010.

[13] M. Takagi, K. Yamaji, and H. Yamamoto, "Power system stabilization by charging power management of plug-in hybrid PHEVS with LFC signal", Proc. of IEEE Vehichle Power Propulsion Conf., pp. 822-826, 2009.

[14] S. Vachirasricirikul and I. Ngamroo, "Robust LFC in a Smart Grid with Wind Power Penetration by Coordinated V2G Control and Frequency Controller", IEEE Transactions on Smart Grid, vol. 5, no. 1, pp. 371-380, 2014.

[15] D. Griffiths, "Pit Construction by Ant-Lion Larvae: A Cost-Benefit Analysis", The Journal of Animal Ecology, vol. 55, no. 1, p. 39, 1986.

[16] H. Shayeghi, A. Molaee, and K. Valipour, "Multi-source power system FOPID based load frequency control with high-penetration of distributed generations", Proc. of Electrical Power Distribution Networks Conference, pp. 131-136, 2016.

BIOGRAPHIES

Hossein Shayeghi received the B.S. and M.S.E. degrees in Electrical and Control Engineering in 1996 and 1998, respectively. He re ceived his Ph.D. degree in Electrical Engineering from Iran University of Science and Technology, Tehran, Iran in 2006. Currently, he is a full Professor in Technical Engineering Department of University of Mohaghegh Ardabili, Ardabil, Iran. His research interests are in the application of robust control, artificial intelligence and heuristic optimization methods to power system control design, operation and planning and power system restructuring. He has authored and co-authored of 6 books in Electrical Engineering area all in Farsi, one book and four book chapters in international publishers and more than 350 papers in international journals and conference proceedings. Also, he collaborates with several international journals as reviewer boards and works as editorial committee of three international journals. He has served on several other committees and panels in governmental, industrial, and technical conferences. He was selected as distinguished researcher of the University of Mohaghegh Ardabili several times. In 2007 and 2010 he was also elected as distinguished researcher in engineering field in Ardabil province of Iran. Furthermore, he has been included in the Thomson Reuters' list of the top one percent of most-cited technical Engineering scientists in 2015 and 2016, respectively. Also, he is a member of Iranian Association of Electrical and Electronic Engineers (IAEEE) and senior member of IEEE.

Masoud Mohammadzadeh received B.S degree in Electrical Engineering from Faculty of Technical Eng. Iran in 2014. Currently He is a M.S.E. student in Technical Eng. Department of the University of Mohaghegh Ardabili, Ardabil, Iran. His areas of interest are application of vehicle-to-grid technology, modeling of batteries.

Seyed-Jalal Seyed-Shenava was born in Ardabil/Iran. He received his B.Sc. in Electrical Engineering from Tehran University in 1991, and his M.SC. and Ph.D. in Electrical Power Engineering both from TMU (Tarbiat Modares University), Tehran/Iran in 1995 and 2008, respectively. Since 1995, he has been with University of Mohaghegh Ardabili, Ardabil/Iran where he is currently an Assoc. professor. His research interests are electricity planning, operation and reliability of power systems.

Rashid Dadkhah Doltabad Received the B.S. Degree in Electrical Engineering from Mazandarann University, Babol Branch, and the M.S.E. degree in Electrical Engineering Department of slamic Azad University, Ardabil Branch. His areas of interest are research on Power System Operation.